Experimental Investigation of the Mean Flow of the Laminar Supersonic Cone Wake

DENNIS K. MCLAUGHLIN,* JAMES E. CARTER,† MORTON FINSTON,‡ AND J. ALAN FORNEY§
Massachusetts Institute of Technology, Cambridge, Mass.

The mean flow of the near wake of a sharp, 7° half-angle, adiabatic cone at Mach number 4.3 and freestream Reynolds numbers of 40,600 and 94,300 was studied experimentally. The cone was supported by a 5-degree-of-freedom magnetic model suspension system. Measurements were made of Pitot pressure, static pressure (using both cone and cone-cylinder static pressure probes), and recovery temperature of a hot-film probe in the near wake region between the model and six model diameters downstream. This enabled the flow regions to be mapped and a complete determination of the flowfield properties at the measurement stations excluding the interior region of the recirculation bubble. The near wake was fully laminar at a Reynolds number of 40,600, and at the higher Reynolds number of 94,300 the flow downstream of the recirculation region underwent transition to turbulence. When compared with hypersonic cone wake measurements, it was shown that the recirculation region was two or three times longer at the lower Mach number, and the pressure overshoot peculiar to the hypersonic cone wake was not found in the present measurements.

Nomenclature

C = Chapman-Rubesin constant = μ_w/μ_{orig} (T_{orig}/T_w)
d = cone model base diameter (sometimes probe diameter)
M = Mach number
p = static pressure
p_b = base pressure
p_c = cone probe pressure
p_p = Pitot pressure
p_s = cone-cylinder probe pressure (needle probe)
r = radial coordinate
Re = Reynolds number
T = temperature
u = x component of velocity
x = longitudinal coordinate
y = vertical coordinate
z = horizontal coordinate
η^2 = $2\int_0^r T_e/T\ r dr$, stretched radial coordinate in wake
ρ = density
Φ_p = angle of yaw of probe *wrt* local flow
$\bar{\chi}$ = hypersonic interaction parameter = $C^{1/2}M^3_{orig}/Re_{orig}^{1/2}$

Subscripts

c_L = centerline
e = edge of viscous region
h = cone medel base radius
l = cone length
m = measured
0 = stagnation condition
w = wall
∞ = freestream condition
orig = condition just outside the boundary layer

Received May 15, 1970; revision received September 28, 1970. This research was supported by the U.S. Air Force, Office of Scientific Research under Contract F44620-69-C-0013.

* Graduate Student; presently Assistant Professor, School of Mechanical and Aerospace Engineering, Oklahoma State University, Stillwater, Okla. Associate Member AIAA.

† Graduate Student; presently Aerospace Engineer, NASA Langley Research Center, Hampton, Va. Member AIAA.

‡ Professor of Aeronautics and Astronautics. Associate Fellow AIAA.

§ Graduate Student; presently Aerospace Engineer, Aerophysics Division, NASA Manned Space Flight Center, Huntsville, Ala.

Introduction

A SUBSTANTIAL literature on experiments of supersonic and hypersonic wakes has accumulated in the past several years. As a result of the interest in re-entry vehicles, much of this work is concentrated on high Mach numbers. Many two-dimensional wake flowfields have been fully determined experimentally—namely, the flowfields around circular cylinders and wedges at $M_\infty \simeq 6$.[1-3] In these cases the wakes have been almost totally laminar. Measurements in axisymmetric wakes have been far less detailed due to the obvious support problem. For fully turbulent cases, detailed flowfield measurements have been made by Ragsdale and Darling[4] and by Martelucci et al.[5] in supersonic/hypersonic axisymmetric wakes. Comparison of wakes behind free-fall models to those of wire-supported models by Dayman[6] indicate that the aforementioned fully turbulent wakes are less affected by support interference than laminar wakes.

In the laminar hypersonic cone wake a wide Mach number range has been covered by experiments. Ballistic ranges[7] and shock tunnels[8] have been used, and recently published detailed flowfield measurements by Murman[9] have been performed in an $M_\infty = 16$ wind tunnel using magnetic model suspension.

In the laminar case, significant changes in the near wake structure occur between the low supersonic Mach numbers and about Mach number 7 where hypersonic freeze appears to take effect. Outside the MIT Aerophysics Laboratory, detailed measurements have not been made in the laminar supersonic cone wake in the absence of support interference. The present investigation was undertaken to study this wake from the model base to six diameters downstream. (For a schematic of the flowfield see Fig. 1.) A unique feature of the facility is the magnetic model suspension system. This system is operated in conjunction with a Mach number 4.3 continuous flow wind tunnel. The range of unit Reynolds numbers available (from 50,000 to 500,000/in.) includes the regime in which the near wake is fully laminar and the regime in which small Tollmien-Schlichting-like oscillations first amplify. The behavior of the instability waves has been investigated and is reported in McLaughlin.[10]

In order to uniquely determine the mean flowfield, three independent measurements must be made. The group of measurements performed in this investigation was Pitot

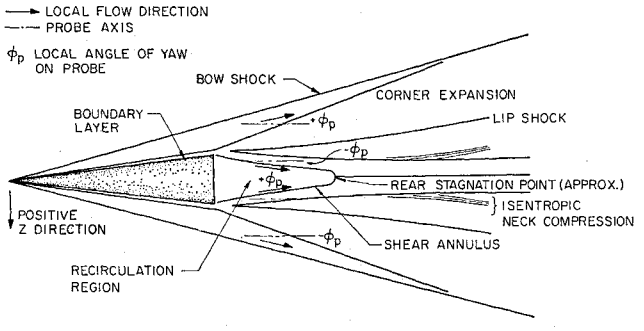

Fig. 1 Near wake map at $M_\infty = 4.30$, $Re_{\infty d} = 40{,}600$.

pressure, static pressure, and hot-film recovery temperature. The reasons for not using the hot-wire heat loss measurement are outlined in Ref. 10.

Prior to this investigation, static pressure probes had not been used with total success in the laminar near wake because of the probe angulation error. In this experimental program, two types of static pressure probes were constructed which eliminated, to a large extent, the angulation error. Details of the design of these probes (the cone probe and cone-cylinder probe) are discussed in Ref. 11. The two static pressure measurements provided two groups of three independent measurements, therefore providing a useful redundancy in the data reduction.

Naturally, the reverse flow regions of the recirculation region are not fully determined because the pressure probes point in the opposite direction from the flow. Here the uncertainties in the measurements are also much higher because of the low pressure levels. However, the boundary of the recirculation region and the full flowfield downstream of the rear stagnation point (see Fig. 1) are determined with acceptable accuracy.

Description of Experiment

Flow Conditions

The experiments were performed in the MIT Aerophysics Laboratory Gas Dynamics Facility using the nominal $M = 4.3$ nozzle. This tunnel is of the continuous flow, open jet type with a test section area 3×3.8 in. The usable core of inviscid flow is approximately 2.3×3 in. For the experiments reported here the stagnation temperature was maintained at 250°F and the stagnation pressure was set at 12 psia and 27 psia. This resulted in Reynolds numbers based on model base diameter of 40,600 and 94,300. Hot-wire fluctuation measurements showed that at $Re_{\infty d} = 94{,}300$, transition to a turbulent inner wake occurred just downstream of the neck.

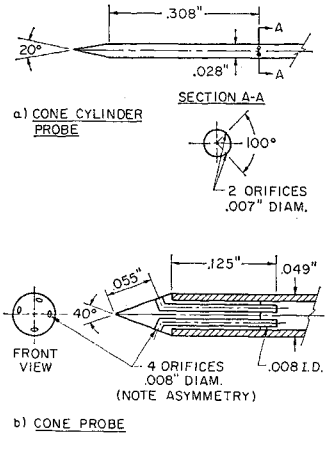

Fig. 2 Details of the static pressure probes.

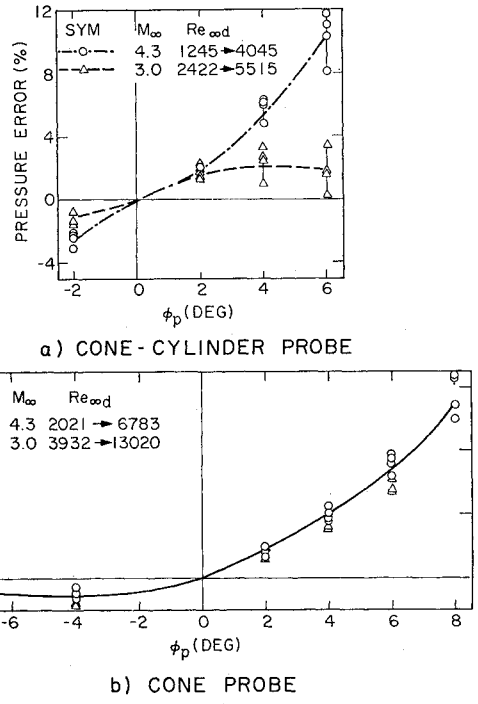

Fig. 3 Results of static pressure probes angulation experiments.

Models and Model Suspension Systems

The models were all 7° half-angle cones with a sharp point (ratio of nose radius to base radius less than 0.01) and a length of 3 in. The cones were very close to adiabatic wall temperature. For freestream Mach numbers around 4.3 the resulting ratio of model temperature to freestream stagnation temperature is about 0.88. The models were supported with a 5-degree-of-freedom magnetic suspension system, which is described in Ref. 12. The suspension system is capable of balancing a model at a predetermined position within ±0.005 in. and to a given angle of attack within ±0.3° (part of which is systematic error). The angle-of-attack set point can be changed by as much as 5°. This capability is used during run conditions to examine (for example) the traverses of Pitot pressure and to vary the angle-of-attack set point until the profiles appear reasonably symmetric. In this way the model angle of attack can be set to zero within ±0.2° (essentially removing the systematic error). For a detailed explanation, see Ref. 10.

Instrumentation and Data Reduction Technique

The behavior of the probes used in the experiments was considered by Forney[13] for the full Mach number and Reynolds number regimes encountered in the supersonic cone near wake. He devised two computational schemes based on input data of Pitot pressure, hot-film recovery temperature, and two static pressure measurements. Some of the details of his programs were modified for convenience,[10] but his basic convergence schemes were retained.

For the most part, the Pitot pressure measurements were completed in 1967.[14] The construction of the probes, which are essentially square-ended glass tubes drawn down to about 0.013 in. o.d. at the tip, is described therein. Additional Pitot pressure measurements were made (in particular, along the model axis) in the present program, using a new pressure transducer with significantly better accuracy (Statham PA 208 TC 5 psi.). Calibration data of Matthews[15] and Sherman[16] was used to make viscous corrections to the Pitot pressure measurements.

The details of the static pressure probes are discussed in Ref. 11 and are shown in Fig. 2. The two types of probes, the cone-cylinder (referred to as the needle probe) and cone static pressure probes, were designed with consideration of the four major sources of systematic error: 1) probe interference, 2) probe angularity, 3) viscous interaction, and 4) time response. Measurements indicated that probe interference and time response do not cause significant errors with the final probe designs. The asymmetry in orifice location of the cone probe was unintentional, but proved to be useful when the angulation calibration experiments were analyzed.

The viscous interaction behavior of the cone-cylinder probe should be the same as that found by Behrens,[17] since, from this viewpoint, the probe was designed exactly as his. The viscous interaction behavior of the cone probe was established with calibration experiments.[11] In the case of both probes the viscous error was correlated with the hypersonic viscous interaction parameter $\bar{\chi}$. The error is proportional to the cube of the Mach number and thus diminishes quickly for lower Mach numbers. As a result, low Mach number portions of the flow cause little viscous error, and it is assumed that subsonic portions cause none.

For the data reduction procedure at transonic and high subsonic Mach numbers, the experimental work of Solomon[18] and of Capone[19] was used to predict the behavior of the cone-cylinder and cone static pressure probes, respectively. Calculations at the lower subsonic Mach numbers were discarded since measurement uncertainties for this flow regime were unreasonably high. As a result, the computed properties are not calculated for the inner region of the recirculation bubble.

Additional calibration experiments were performed with both static pressure probes to establish sensitivity to flow angulation at supersonic Mach numbers. The results of these experiments are presented in Fig. 3 and discussed in Ref. 11. Reference to the calibration results is made in preparation of the data for input to the data reduction programs.

Total temperature was measured with a hot-film probe (Thermal Systems Inc. probe No. 1276-10) of the same configuration as a hot-wire. The advantage of the hot-film is almost complete elimination of the end-loss error over the range of Knudsen numbers encountered in the calibration experiments. Measurements in a known flow with the hot-film probe fall right on the infinite wire correlation curve of Dewey[20] indicating that the end-loss correction, which must be included when the hot-wire is used, is no longer necessary. (See Ref. 10 for a full discussion of this point.)

All measurements were made by driving the probe horizontally or vertically through the axis of symmetry of the model, each traverse extending about $\pm 1.5d$ from the model axis. The $-z$ direction profile is referred to as the horizontal mirror image of the $+z$ direction profile. An indication of the symmetry in the flowfield is obtained by viewing an overlay of the $-z$ and $+z$ profiles. Since the model angle of attack was zero, a horizontal and vertical traverse yields four profiles when plotted vs the coordinate r.

Experimental Results

Static Pressure Measurements

The results of the cone-cylinder static pressure measurements are presented in Ref. 11. An additional composite is shown in Fig. 4 in which the horizontal profiles are compared with their mirror images for $Re_{\infty d} = 94{,}300$. Using the sign convention shown in Fig. 1 along with the results of the angulation experiments, an attempt was made to establish whether or not the profile differences in Fig. 4 were due to flow angulation. In general, the behavior was inconsistent since the differences were so small that random errors due to model drift and small-scale jet irregularities dominated. The profile used for input data to the computer program is a simple average of all the horizontal and vertical profiles.

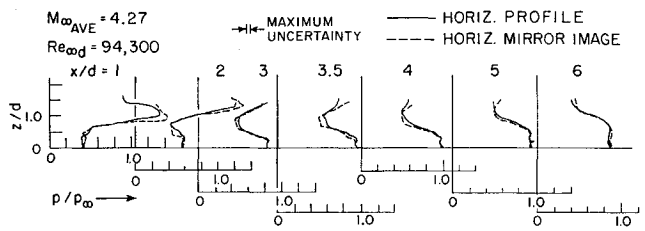

Fig. 4 Cone-cylinder static pressure measurements at $Re_{\infty d} = 94{,}300$.

The results of cone static pressure measurements are presented in Ref. 11. In addition, as with the cone-cylinder static pressure measurements, a composite comparing horizontal mirror image profiles is shown in Fig. 5. In this case differences between the profiles can be attributed in a consistent manner to the probe angulation error. A crossover point is marked with a star on each profile. Outside this radius there is positive yaw on the probe during the horizontal mirror image profile and negative yaw during the horizontal profile. Inside the starred radius the opposite is true. (refer to Fig. 1). Note that in nearly every profile the pressure measurements reflect the positive error with positive yaw result of the calibration data. The final two profiles do not indicate this behavior, since this far downstream the flow is nearly parallel, and systematic jet irregularities, mainly caused by disturbances which propagate inwards from the jet edge, are larger.

The calibration experiments indicated less than 2% flow angulation errors for the cone probe from 0 to 8° negative angle of yaw. Hence the outer segment from the horizontal profile and the inner segment from the horizontal mirror image profile were selected for input to the data reduction program. (See Ref. 10 for more details.)

Pitot Pressure Measurements and Location of Rear Stagnation Point

The results of Pitot pressure measurements at $Re_{\infty d} = 40{,}600$ are presented in Ref. 14. Repeat measurements were made in 1968 with the improved transducer system to obtain measurements with less uncertainty in and around the recirculation region. With these improved measurements, the rear stagnation point can be located with reasonable accuracy (see Fig. 6) by comparing the axial distributions of Pitot pressure with cone static and cone-cylinder static pressure. (This technique was also used by Batt and Kubota.[3]) Moving upstream, the point where the pressure measurements first coincide should be the rear stagnation point. In this case, a good estimate of this point is 2.5 model diameters downstream of the base for both Reynolds number cases.

The laminar supersonic cone wake is peculiar in having such a long recirculation region. Martellucci et al.[5] have correlated a number of axisymmetric and two-dimensional laminar and turbulent wake measurements covering wide Mach and

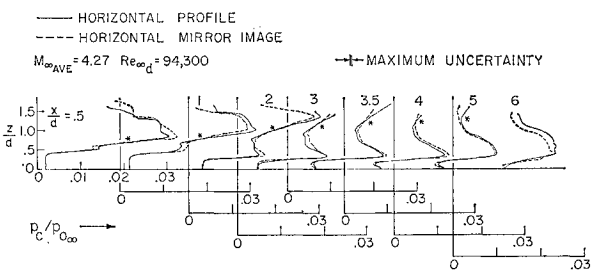

Fig. 5 Cone static pressure measurements at $Re_{\infty d} = 94{,}300$.

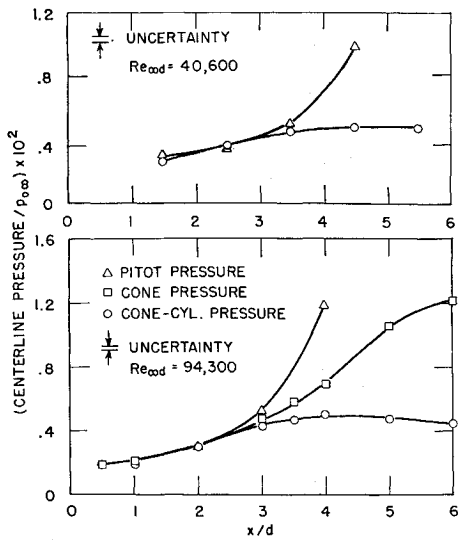

Fig. 6 Pitot, cone static, and cone-cylinder static pressure axial distributions in near wake.

Reynolds number ranges. They find the rear stagnation points for all cases to be around 0.8 diam downstream of the base. However, for freestream Mach numbers less than about 5, Martellucci et al. have included no data on laminar wakes. The flowfield geometry shown in Fig. 1, which was obtained from the present measurements, is in good agreement with Schlieren photographs by King[21] and by Dayman[6] of free-flight cone wakes at the lower Mach numbers. The noteworthy agreement comes in the shape of the long recirculation bubble.

Total Temperature Measurements

The hot-film recovery temperature raw data was presented in Ref. 11. Included here is the data for the low Reynolds number case which had gross asymmetries much more pronounced than the data for $Re_{\infty d}$ = 94,300 (Fig. 7). The cause of these asymmetries was not known at the time Ref. 11 was published, but since that time experiments have been performed which prove that the effect was not caused by probe interference, but rather was due to systematic jet irregularities. (The maximum variation in freestream Mach number is ±2%.) In particular, these irregularities are caused by the imbalance of pressure between the open jet and its surroundings. It was demonstrated in Ref. 10 that the wake asymmetry was very sensitive to the jet expansion outside its exit Mach rhombus. The horizontal and vertical traverses differ because the expansion waves from the sides of the nozzle exit intersect the wake axis upstream of those from the top and bottom of the nozzle due to the rectangular cross section. The asymmetry could be almost removed by a careful balancing of the jet static pressure with the surrounding pressure. It was not practical for all data acquisition to run in a null pressure balance condition, however, since the tunnel flow was very unstable in this condition (tending to shock down to subsonic flow).

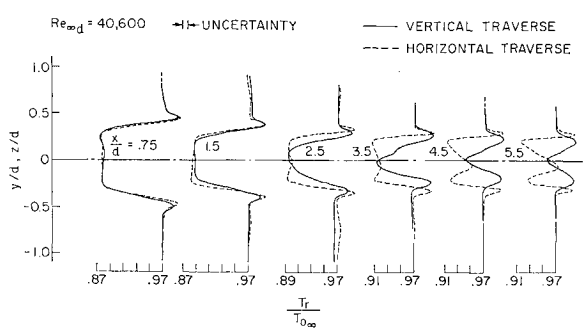

Fig. 7 Hot-film recovery temperature measurements at $Re_{\infty d}$ = 40,600.

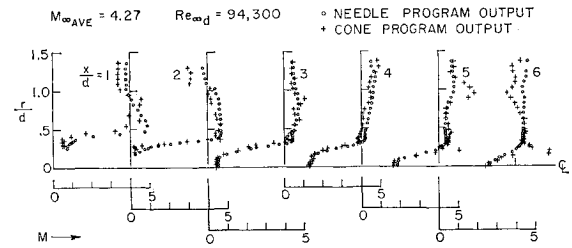

Fig. 8 Calculated Mach number profiles for $Re_{\infty d}$ = 94,300.

The hot-film recovery temperature profiles are the measurements most affected by the jet underexpansion. It is not understood why they should be affected more than the pressure measurements. There is a small asymmetry present in the cone static pressure measurements, a barely detectable asymmetry in some Pitot measurements, and no asymmetry at all in some Pitot and all cone-cylinder static pressure measurements. Empty jet temperature measurements showed no gross irregularities.

The asymmetry in the temperature measurements is removed by averaging horizontal and vertical profiles before inputting to the computer program. This seems reasonable in view of its obvious assignable cause. Fortunately, the added uncertainty in the data is not amplified in the data reduction programs.

Computed Results and General Discussion

Calculated Mach number profiles for the Reynolds number 94,300 case are shown in Fig. 8 for a comparison of the output data of the two data reduction programs. The two programs have independently measured inputs, and the good agreement between the data is strong evidence that the measurements are reliable.

The exceptions to the good agreement between the calculated Mach numbers from the two programs occur in the shear annulus and close to the lip shock. At these radial positions the cone data must be suspect because the resolution is so much poorer with the cone probe due to its larger diameter. For example, the shear annulus can be as thin as 0.10 in. compared with the cone probe diameter of 0.049 in.

In general the small-scale fluctuations in the cone program output are larger than in the smooth needle program output. An error analysis of the two computation schemes clarifies this point. The outputs of the cone program are much more sensitive than are the outputs of the needle program. It is significant that, although the cone pressure can be measured more accurately than cone-cylinder (needle) static pressure due to the higher pressure level, the calculated quantities from the cone program have much larger uncertainties. The uncertainty of each calculated quantity varies with the local

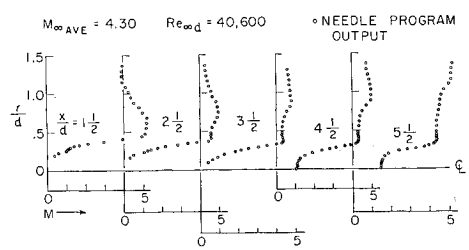

Fig. 9 Calculated Mach number profiles for $Re_{\infty d}$ = 40,600.

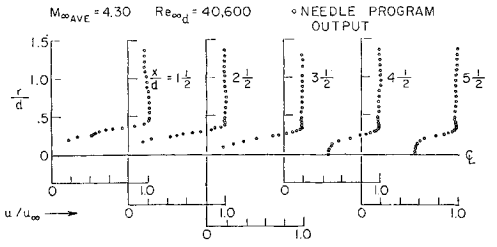

Fig. 10 Calculated velocity profiles for $Re_{\infty d}$ = 40,600.

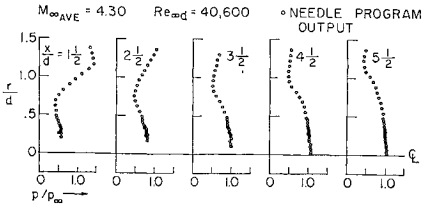

Fig. 12 Calculated static pressure profiles for $Re_{\infty d}$ = 40,600.

flow conditions as was shown in the error analysis of Ref. 10. In the supersonic portions of the flow, each calculated quantity from the needle program has an uncertainty of less than ±10%; however, the cone program results have larger uncertainties—upwards of 20%. For this reason the output data from the needle program will be accepted as representing the true values. At $Re_{\infty d}$ = 40,600 the uncertainty amplification in the cone program data reduction becomes even larger, due to the large viscous interaction correction made to the cone static pressure. Hence the results of the cone program for $Re_{\infty d}$ = 40,600 were in general unreliable and are not presented here.

Figure 9 shows the calculated Mach number distributions behind the cone for the $Re_{\infty d}$ = 40,600 case. Comparison with the profiles of the $Re_{\infty d}$ = 94,300 case (Fig. 8) reveals very little difference upstream of the rear stagnation point. The two and one half fold increase in Reynolds number produces a thinning of the shear annulus and minimum wake width, as expected. However, the striking difference in the two cases comes downstream of the recirculation region. At $Re_{\infty d}$ = 94,300 the rapid decay of the Mach number defect indicated an obvious departure from laminar behavior. On the other hand, at the lower Reynolds number laminar case, the slow decays indicate that the momentum defect and high temperature will persist many diameters downstream. (See Figs. 10–12 for the calculated velocity, temperature, and static pressure profiles at $Re_{\infty d}$ = 40,600.)

In a prior publication,[14] along with the detailed Pitot pressure measurements, we presented a discussion of the qualitative nature of the cone near wake flowfield. It is appropriate to mention the salient points of that discussion as well as some new observations at this time. The obviously longer recirculation region (smaller closure angle) changes all of the flow geometry somewhat. The lip shock, shown to be very weak for these conditions,[14] does not intersect the neck shock until far downstream of the neck (unlike in the hypersonic wedge wake).[3] In our measurements—as far back as six base diameters—there is only a smooth compression returning the outer inviscid flow back to the freestream direction. A neck shock must eventually appear downstream as a result of the confluence of compression waves.

From the Pitot pressure surveys[14] a region of constant Pitot pressure between the shear annulus edge and the lip shock is observed. This indicates that the large region of inviscid rotational flow, resulting from a tremendous divergence of streamlines originally in the cone boundary layer, and

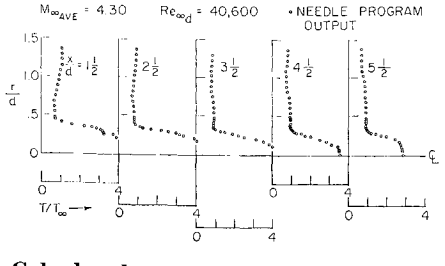

Fig. 11 Calculated tmeperature profiles for $Re_{\infty d}$ = 40,600.

so prominent in hypersonic wakes, is not present in the supersonic case.

Examining the static pressure along the model axis downstream of the rear stagnation point (Fig. 12), we do not find the pressure overshoot found by Murman[9] and predicted by the theory of Weiss et al.[22] for hypersonic wakes. The static pressure profiles also show it is a good approximation to assume constant static pressure in the radial direction from the axis out to the edge of the high shear region. This is also true in the recirculation region within the accuracy of the measurements (also seen in the raw cone-cylinder static pressure data of Fig. 4). Although the pressure is reasonably constant in the radial direction, strong gradients are present in the axial direction. This would indicate a general approach using boundary-layer equations would be fruitful. Such an approach has been taken by Ohrenberger and Baum,[23] which is the most complete (and most recent) theoretical approach to the near wake problem. Their calculations, however, covering both two-dimensional and axisymmetric situations were performed for a high Mach number (hypersonic) laminar wake, as were the calculations of earlier theoretical works.[22,24,25] This difference makes it difficult to make comparisons between our measurements and their theoretical predictions.

One useful comparison examines measured velocity profiles downstream of the rear stagnation point with Gaussian profiles (for shape only), which are used in the work of Finson and Weiss.[24] Figure 13 compares measured profiles of velocity with Gaussians at the axial positions of 4.5 and 5.5 diam for the fully laminar Reynolds number case ($Re_{\infty d}$ = 40,600). Experimental data is plotted vs the stretched radial coordinate η, which is the Dorodnitsyn-Howarth variable. It is clear that these profiles have not yet developed into Gaussians. They are closer to the top hat profile, indicating that the upper and lower shear layers have not fully coalesced.

Summary and Conclusions

Measurements with the cone-cylinder and cone static pressure probes appear to be accurate since errors due to probe angulation are acceptably small. Use of the hot-film probe for total temperature measurements introduces a substantial simplification in this application.

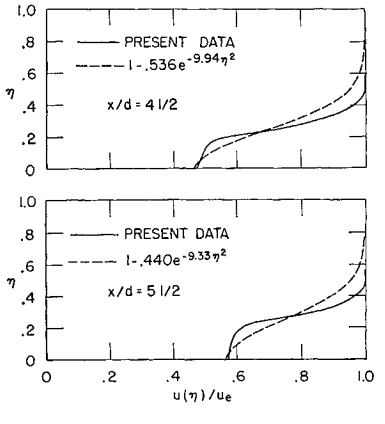

Fig. 13 Comparison of measured velocity profiles with Gaussians.

The flowfield is mapped except for the reverse flow regions. Comparison of the results of data reduction programs using two groups of measured quantities shows close agreement, providing strong evidence that the measurements are reliable.

Some differences between the supersonic cone wake and hypersonic cone wake are established. The length of the recirculation region is significantly longer at the lower Mach numbers. As a result, the large static pressure overshoots present in hypersonic cone wakes are not found in the supersonic case. In addition, the radial static pressure variation from the axis to the edge of the viscous region is negligible both in the recirculation region and downstream in the inner wake.

References

[1] Dewey, C. F., Jr., "Near Wake of a Blunt Body at Hypersonic Speeds," *AIAA Journal*, Vol. 3, No. 6, June 1965, pp. 1001–1010.

[2] Behrens, W., "The Far Wake Behind Cylinders at Hypersonic Speeds—Part I Flow Field," *AIAA Journal*, Vol. 5, No. 12, Dec. 1967, pp. 2135–2141.

[3] Batt, R. G. and Kubota, T., "Experimental Investigation of Laminar Near Wakes Behind 20° Wedges at $M_\infty = 6$," *AIAA Journal*, Vol. 6, No. 11, Nov. 1968, pp. 2077–2083.

[4] Ragsdale, W. C. and Darling, J. A., "An Experimental Study of the Turbulent Wake Behind a Cone at Mach 5," TR 66-95, 1966, Naval Ordnance Laboratory, White Oak, Md.

[5] Martellucci, A., Trucco, H., and Agone, A., "Measurements of the Turbulent Near Wake of a Cone at Mach 6," *AIAA Journal*, Vol. 4, No. 3, March 1966, pp. 385–391.

[6] Dayman, B., Jr., "Support Interference Effects on the Supersonic Wake," *AIAA Journal*, Vol. 1, No. 8, Aug. 1963, pp. 1921–1922.

[7] Pallone, A. J., Erdos, J. I., and Eckerman, J., "Hypersonic Laminar Wakes and Transition Studies," *AIAA Journal*, Vol. 2, No. 5, May 1964, pp. 855–863.

[8] Cresci, R. J. and Zakkay, V., "An Experimental Investigation of the Near Wake of a Slender Cone at $M_\infty = 8$ and 12," *AIAA Journal*, Vol. 4, No. 1, Jan. 1966, pp. 41–46.

[9] Murman, E. M., "Experimental Studies of a Laminar Hypersonic Cone Wake," *AIAA Journal*, Vol. 7, No. 9, Sept. 1969, pp. 1724–1730.

[10] McLaughlin, D. K., "Experimental Investigation of the Mean Flow and Stability of the Laminar Supersonic Cone Wake," Ph.D. thesis, Nov. 1969, MIT, Cambridge, Mass.; also *AIAA Journal*, Vol. 9, No. 4, April 1971.

[11] McLaughlin, D. K., Carter, J. E., and Finston, M., "Experimental Investigation of the Near Wake of a Magnetically Suspended Cone at $M_\infty = 4.3$," AIAA Paper 69-186, New York, 1969.

[12] Tilton, E. L., et al., "The Design and Initial Operation of a Magnetic Model Suspension and Force Measurement System," *Journal of the Royal Aeronautical Society*, Vol. 67, Nov. 1963, pp. 717–744.

[13] Forney, J. A., "Computer Program for Hypersonic Wake Data Processing," S. M. thesis, Nov. 1968, MIT, Cambridge, Mass.

[14] Browand, F. K., Finston, M., and McLaughlin, D. K., "Wake Measurements Behind a Cone Suspended Magnetically in a Mach Number 4.3 Stream," CP 19, May 1967, AGARD.

[15] Matthews, M. L., "An Experimental Investigation of Viscous Effects on Static and Impact Pressure Probes in Hypersonic Flow," Memo 44, June 1958, GALCIT, Hypersonic Research Project, Pasadena, Calif.

[16] Sherman, F. S., "New Experiments on Impact-Pressure Interpretation in Supersonic and Subsonic Rarefied Air Streams," TN 2995, 1953, NACA.

[17] Behrens, W., "Viscous Interaction Effects on a Static Pressure Probe at $M = 6$," *AIAA Journal*, Vol. 1, No. 12, Dec. 1963, pp. 2364–2366.

[18] Solomon, G. E., "Transonic Flow Past Cone Cylinders," Rept. 1242, 1955, NACA.

[19] Capone, F. J., "Wind Tunnel Tests of Seven Static-Pressure Probes at Transonic Speeds," TN-D-947, Nov. 1961, NASA.

[20] Dewey, C. F., Jr., "A Correlation of Convective Heat Transfer and Recovery Temperature Data for Cylinders in Compressible Flow," *International Journal of Heat and Mass Transfer*, Vol. 8, 1965, pp. 245–252.

[21] King, H. H., "Some Base Flow Closure Angle Results for Cones in Free Flight," Research Note 21, 1964, Electro-Optical Systems, Inc., Pasadena, Calif.

[22] Weiss, R., Finson, M., and Greenberg, R., "The Axisymmetric Hypersonic Near Wake with Base Injection," AIAA Paper 69-66, New York, 1969.

[23] Ohrenberger, J. T. and Baum, E., "A Theoretical Model of the Near Wake of a Slender Body in Supersonic Flow," AIAA Paper 70-792, Los Angeles, 1970.

[24] Finson, M. L. and Weiss, R. F., "A Theoretical Investigation of the Hypersonic Axisymmetric Near Wake Recompression Region," Research Rept. 334, July 1969, Avco Everett Research Lab., Everett, Mass.

[25] Reeves, B. L. and Buss, H. M., "Theory of the Laminar Near Wake of Axisymmetric Slender Bodies in Hypersonic Flow," AVMSD-0122-69-RR, Feb. 1969, Avco Missile Systems Div., Wilmington, Mass.